

# Highly Anisotropic Luminescence from Poly(9,9-dioctylfluorene) Nanowires Doped with Orientationally Ordered $\beta$ -phase Polymer Chains

*Deirdre O'Carroll,<sup>†</sup> Gareth Redmond<sup>‡\*</sup>*

Tyndall National Institute, Lee Maltings, Prospect Row, Cork, Ireland.

**RECEIVED DATE (to be automatically inserted)**

\*Corresponding author. [gareth.redmond@ucd.ie](mailto:gareth.redmond@ucd.ie)

<sup>†</sup>Current address: Thomas J. Watson Laboratory of Applied Physics, California Institute of Technology, 1200 E. California Blvd., MC 128-95, Pasadena, CA 91125, USA.

<sup>‡</sup>Current address: School of Physics and School of Chemistry and Chemical Biology, University College Dublin, Belfield, Dublin 4, Ireland.

## Near-Field Optical Imaging and Spectroscopy Setup

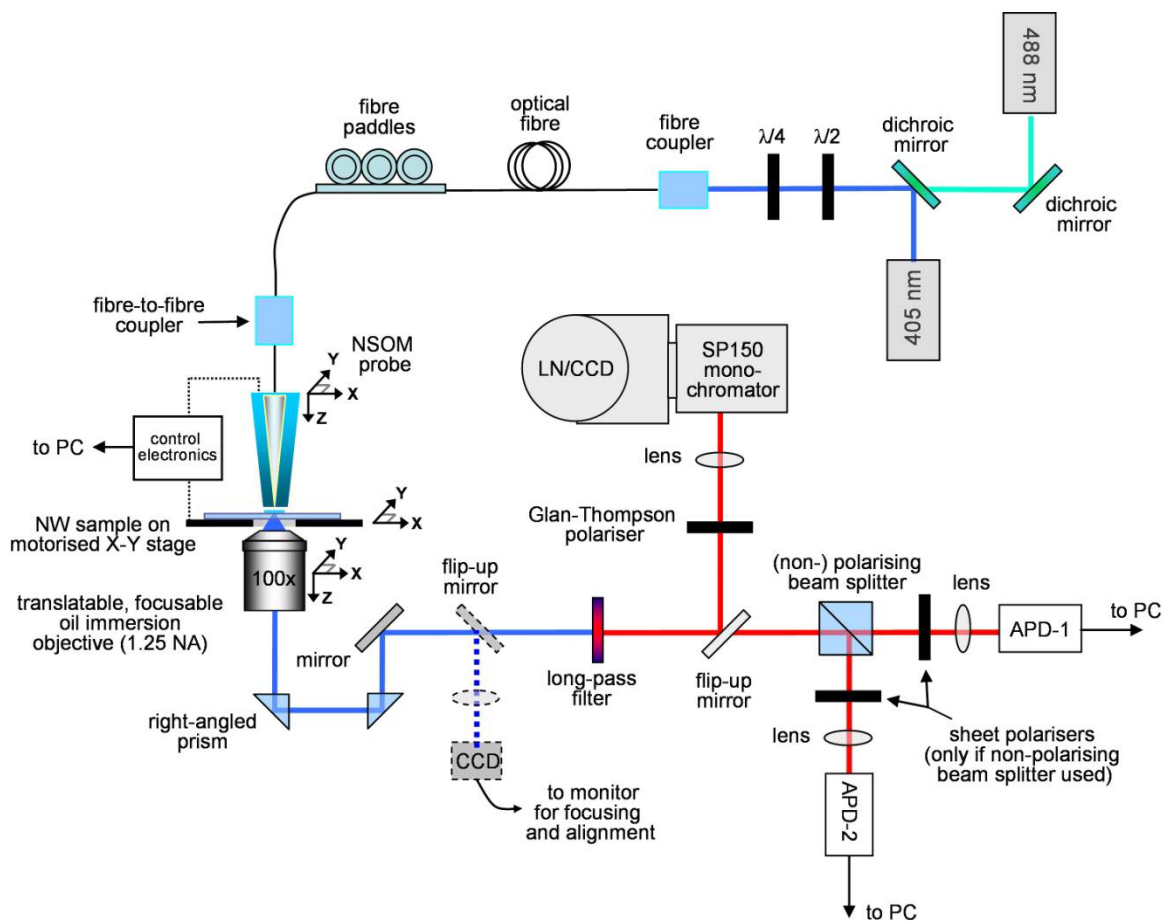


**Figure S1.** Schematic of the optical set-up employed for polarization-resolved near-field optical addressing of single nanowires.

## **Topographic Artifacts and Domains in Aperture NSOM Data**

Any aperture near-field optical study of samples with topographic height variation of more than 10 nm must consider the possibility of topography-induced artifacts.<sup>[S1]-[S7]</sup> Such artifacts result from variations in the distance between the NSOM probe aperture and the sample surface as the tip scans over the sample. These effects are often evident in near-field data acquired under the condition that a constant distance (~ 10 nm) between the NSOM probe tip and the sample surface is maintained during scanning (i.e., constant-gap mode),<sup>[S1]</sup> and are particularly apparent when the NSOM probe has been damaged, resulting in a more blunt probe tip. Hecht *et al.* considered these effects in detail and proposed that, in order for a near-field optical image to be credible, at least one of the following should apply: (1) topography and near-field optical images are highly uncorrelated; (2) correlated structures are displaced by a constant amount indicating that optical and topographic interaction zones do not coincide; (3) the resolution of the topography and PL images are clearly different.<sup>[S1]</sup>

Despite the existence of topographic artifacts, useful information on local chain alignment in emissive conjugated polymer materials may be gained from polarization-resolved aperture fluorescence NSOM studies by taking account of the mechanisms by which topographic artifacts contribute to PL signals and by correct analysis and interpretation of features observed in polarized PL intensity images. Domains exhibiting long-range order may be directly identified in polarization-resolved NSOM PL images when the PL intensities at a location on the sample either anti-correlate or do not correlate at all in two measured orthogonally polarized images. Such variations in PL intensity can be attributed entirely to the properties of the polymer sample rather than to variations in surface topography. Consequently, NSOM-based measurement of polarization-resolved PL data from conjugated polymer materials can provide detailed information about molecular orientation within different domains with high lateral resolution.

For example, Blatchford *et al.* have spatially resolved regions in poly(*p*-pyridyl vinylene) thin films by simultaneously collecting two orthogonally polarized PL images along with the NSOM topography image. Both polarized PL intensity images were found to differ strongly from the topography of the sample and, in addition, the two polarized PL images were clearly different from each other. Hence, the origin of the polarized emission from the sample was attributed to the presence of regions with long-range order.<sup>[S8]</sup> Teetsov *et al.* went a step further and applied fluorescence anisotropy calculations to simultaneously acquired orthogonally polarized NSOM PL images to resolve nanoscale domains of order in as-spun poly(9,9-didodecylfluorene) thin films and thermally annealed poly(9,9-dihexylfluorene) thin films.<sup>[S9],[S10]</sup> In addition, they identified another type of NSOM PL intensity

contrast in as-spun poly(9,9-dihexylfluorene) thin films, namely, cluster-correlated fluorescence, which was attributed to the presence of entangled or insoluble amorphous polymer clumps from solution.

In summary, there are three main contributors to PL intensity contrast in NSOM PL images and their contributions to measured polarized PL images must be considered in detail in order to confidently distinguish between contrast that arises due to the mechanics and dynamics of the measurement system and contrast that arises due to the properties of the sample. Therefore, in order to properly interpret NSOM data acquired from PFO nanowires, the expected contribution of topographic artifacts, cluster-correlated fluorescence and long-range molecular order to measured polarized NSOM PL images will be assessed in the following sections.

### **Topographic Artifacts**

Differences between the NSOM probe tip-sample distance and the NSOM probe aperture-sample distance may be identified as decreases in measured PL intensity in NSOM PL images which correlate with either an increase or a decrease in topographic height. Such topographic artifacts are attributed to the relatively blunt nature of aperture NSOM probes and the nature of the shear force feedback mechanism used to generate topography images. While the NSOM aperture may be 50 - 80 nm in diameter, the actual size of the probe tip is much larger (about 150 to 300 nm in diameter) due to the tapered optical fiber and additional metal cladding which helps confine light exiting the aperture to a very localized region at the tip of the probe. In addition, in constant-gap mode, the shear force feedback mechanism holds the part of the NSOM probe tip that is closest to the sample at a constant distance (of less than 10 nm) from the surface of the sample.

Figure S2 illustrates how the NSOM probe aperture-sample distance ( $h_A$ ) can increase while NSOM probe tip-sample distance ( $h_{SF}$ ) is maintained constant (by shear force feedback) as the NSOM probe scans across a surface with a topographic feature. Figure S2a shows that when the tip is well away from the feature over a flat region of the sample surface, aperture-sample and tip-sample distances are equal. However, when the tip encounters an increase in height at the edge of a topographic feature, the probe retracts in order to maintain a constant tip-sample distance while the aperture-sample distance increases at the edge of the feature, i.e.,  $h_A > h_{SF}$ ; see Figure S2b. When the tip encounters a decrease in height at the edge of the topographic feature, the aperture-sample distance increases again before the tip has time to fully clear the feature; see Figure S2c.

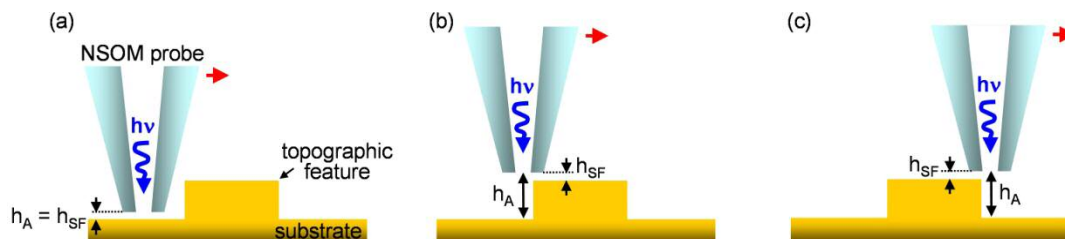


**Figure S2.** Schematic representation of an NSOM probe tip as it scans across a sample surface. (a) The NSOM probe is over a flat region of the surface, well away from any topographic features. (b) The probe encounters an increase in height at the edge of a topographic feature. (c) The probe encounters a decrease in height at the edge of a topographic feature.

Since near-field intensity drops significantly as a function of distance from the NSOM probe aperture, an increase in  $h_A$  results in a decrease in local excitation intensity at the sample surface directly underneath the aperture. Therefore, an increase in aperture-sample distance manifests as a drop in PL intensity measured from the sample. There are numerous examples of such topographic artifacts in the literature.<sup>[S1]-[S7]</sup> Approaches to reduce or eliminate these artifacts include: Constant-height mode imaging;<sup>[S1]</sup> correcting the measured NSOM PL intensities using topographic height information and the tip retraction curve of the NSOM system;<sup>[S11]</sup> use of very sharp NSOM probes.<sup>[S3],[S12]</sup>

### Cluster-Correlated Fluorescence

During NSOM PL analysis of conjugated polymer thin films, insoluble polymer clusters may cause changes in PL intensity from the sample. Although often difficult to distinguish from NSOM topographic artifacts, these features may cause either an increase or a decrease in PL intensity even when NSOM probe aperture-sample distance is maintained constant during scanning. Hence, there is no coupling between the topography and PL signals (even though there may be correlation) since these features are a result of the properties of the sample and not of the NSOM system. However, PL spectra of insoluble clusters are often different to those of the surrounding film due to differing polymer chain configurations or interchain interactions. Nguyen *et al.* employed spatially-resolved NSOM PL spectroscopy to probe nanometer-scale topographic features in spin-cast thin films of poly(2-methoxy-5-(2'-ethylhexyloxy)-1,4-phenylene vinylene).<sup>[S13]</sup> PL spectra acquired from the topographic features were red-shifted in comparison to spectra acquired from the surrounding film. Hence, the features were attributed to regions of the film where the chains were packed more tightly and, consequently, exhibited greater interchain interactions. Also, in studies of other conjugated polymer thin films, insoluble polymer clusters were found to be generally amorphous and, as a consequence, did not exhibit polarized

light emission. This situation was clearly demonstrated by Teetsov *et al.* who detected insoluble clusters in thin films of poly(9,9-dihexylfluorene) by PL NSOM but observed negligible polarization contrast from these features.<sup>[S9]</sup> Since changes in PL intensity at the clusters anti-correlated with topography and correlated in orthogonally polarized NSOM PL images, the term “cluster-correlated fluorescence” was used to describe the resulting intensity variations in NSOM PL images. Prior NSOM studies by DeAro *et al.* of poly(*p*-phenylene vinylene) also detected low PL intensity from clusters in non-oriented polymer thin films, as well as evidence for other domains exhibiting molecular order.<sup>[S14]</sup>

## Long-Range Order

Long-range (i.e., > 50 nm) ordering of polymer molecules, i.e., inter-chain ordering of the molecules with varying degrees of correlation, may also occur within conjugated polymer materials. NSOM PL features arising from long-range order may or may not correlate with features in the sample topography but they may be uniquely identified if the measured PL intensity either anti-correlates or does not correlate at all in orthogonally polarized NSOM PL images. Blatchford *et al.*, Teetsov *et al.*, DeAro *et al.* and Tan *et al.* have each employed polarization-resolved NSOM PL imaging methods to identify such features in conjugated polymer thin films.<sup>[S8]-[S10],[S14],[S15]</sup>

### *Distinguishing Long-Range Order from Topographic Artifacts and Cluster-Correlated Fluorescence*

While NSOM PL signals may suggest the existence of all three feature types (i.e., topographic artifacts, cluster-correlated fluorescence and long-range order) during measurements of conjugated polymer samples, it is possible to decouple long-range order from the other two feature types using polarization-resolved NSOM PL imaging along with fluorescence anisotropy or polarization ratio image calculations. This decoupling of signals can be achieved since features arising from both topographic artifacts and cluster correlated fluorescence always correlate in orthogonally polarized PL images. However, features arising from long-range order either anti-correlate or do not correlate at all. By calculating the local polarization ratio,  $\rho$ , from orthogonally polarized PL images, features that correlate in both PL intensity images will be eliminated while features that anti-correlate or do not correlate will be retained. Figure S3 is a simple illustration of this point. Here a PL intensity line profile acquired under vertically polarized collection conditions (V) is compared with a line profile acquired under horizontally polarized collection conditions (H). Features (i) and (iii) represent the situation whereby the line profiles either anti-correlate or do not correlate, respectively, indicative of long-range order. These features are clearly observed in the calculated polarization ratio profile ( $\rho = (V - H)/(V + H)$ ).

Feature (ii) represents the situation whereby the line profiles measured under both polarizations directly correlate, indicative of the presence of an artifact. Notably, this feature is absent in the  $\rho$  profile since the magnitude of  $\rho$  at this location is the same as that determined for unfeatured regions of the V and H line profiles.

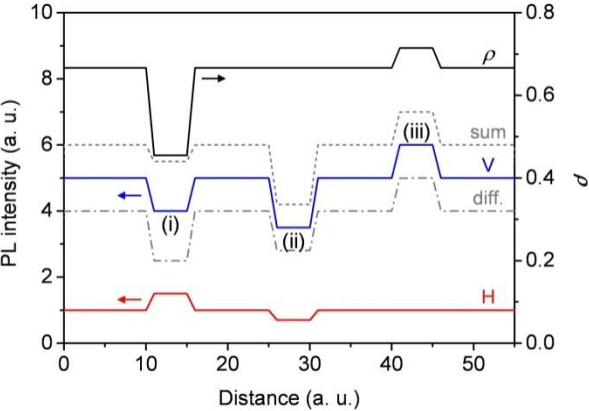


**Figure S3.** Representative plot of two orthogonally polarized PL intensity line profiles (V and H) along with sum (V + H), difference (V – H) and polarization ratio,  $\rho$ ,  $((V - H)/(V + H))$  calculated line profiles.

## References

- [S1] B. Hecht, H. Bielefeldt, Y. Inouye, D. W. Pohl, L. Novotny, *J. Appl. Phys.* **1997**, *81*, 2492-2498.
- [S2] R. L. Williamson, L. J. Brereton, M. Antognozzi, M. J. Miles, *Ultramicroscopy* **1998**, *71*, 165-175.
- [S3] G. Kaupp, A. Herrmann, M. Haak, *J. Phys. Org. Chem.* **1999**, *12*, 797-807.
- [S4] R. Brunner, M. E. Kosal, K. S. Suslick, R. Lamche, O. Marti, J. O. White, *Ultramicroscopy* **2000**, *84*, 149-157.
- [S5] R. Stevenson, R. Riehn, R. G. Milner, D. Richards, E. Moons, D. -J. Kang, M. Blamire, J. Morgado, F. Cacialli, *Appl. Phys. Lett.* **2001**, *79*, 833-835.
- [S6] D. Richards, *Phil. Trans. R. Soc. Lond. A* **2003**, *361*, 2843-2857.
- [S7] X. Wang, Z. Fan, T. Tang, *J. Opt. Soc. Am. A* **2005**, *22*, 2730-2736.
- [S8] J. W. Blatchford, T. L. Gustafson, a. J. Epstein, D. A. Vanden Bout, J. Kerimo, D. A. Higgins, P. F. Barbara, D. -K. Fu., T. M. Swager, A. G. MacDiarmid, *Phys. Rev. B* **1996**, *54*, R3683-R3686.
- [S9] J. Teetsov, D. A. Vanden Bout, *J. Phys. Chem. B* **2000**, *104*, 9378-9387.
- [S10] J. A. Teetsov, D. A. Vanden Bout, *J. Am. Chem. Soc.* **2001**, *123*, 3605-3606.
- [S11] C. E. Jordan, S. J. Stranick, L. J. Richter, R. R. Cavanagh, *J. Appl. Phys.* **1999**, *86*, 2785-2789.
- [S12] H. F. Hamann, A. Gallagher, D. J. Nesbitt, *Appl. Phys. Lett.* **2000**, *76*, 1953-1955.
- [S13] T. Q. Nguyen, B. J. Schwartz, R. D. Schaller, J. C. Johnson, L. F. Lee, L. H. Haber, R. J. Saykally, *J. Phys. Chem. B* **2001**, *105*, 5153-5160.
- [S14] J. A. De Aro, K. D. Weston, S. K. Buratto, U. Lemmer, *Chem. Phys. Lett.* **1997**, *277*, 532-538.
- [S15] C. H. Tan, A. R. Inigo, J. -H. Hsu, W. Fann, P. -K. Wei, *J. Phys. Chem. Solids* **2001**, *62*, 1643-1654.